Precision theoretical analysis of neutron radiative beta decay to order $O(\alpha^2/\pi^2)$

A. N. Ivanov,[1,*] R. Höllwieser,[1,2,†] N. I. Troitskaya,[1,‡] M. Wellenzohn,[1,3,§] and Ya. A. Berdnikov[4,‖]

[1]*Atominstitut, Technische Universität Wien, Stadionallee 2, A-1020 Wien, Austria*
[2]*Department of Physics, New Mexico State University, Las Cruces, New Mexico 88003, USA*
[3]*FH Campus Wien, University of Applied Sciences, Favoritenstraße 226, 1100 Wien, Austria*
[4]*Peter the Great St. Petersburg Polytechnic University, Polytechnicheskaya 29, 195251, Russian Federation*

(Received 28 April 2017; published 26 June 2017)

In the Standard Model (SM) we calculate the decay rate of the neutron radiative β^- decay to order $O(\alpha^2/\pi^2 \sim 10^{-5})$, where α is the fine-structure constant, and radiative corrections to order $O(\alpha/\pi \sim 10^{-3})$. The obtained results together with the recent analysis of the neutron radiative β^- decay to next-to-leading order in the large proton-mass expansion, performed by Ivanov *et al.* [Phys. Rev. D **95**, 033007 (2017)], describe recent experimental data by the RDK II Collaboration [Bales *et al.*, Phys. Rev. Lett. **116**, 242501 (2016)] within 1.5 standard deviations. We argue a substantial influence of strong low-energy interactions of hadrons coupled to photons on the properties of the amplitude of the neutron radiative β^- decay under gauge transformations of real and virtual photons.

DOI: 10.1103/PhysRevD.95.113006

I. INTRODUCTION

During a long period the radiative β^- decay of a free neutron $n \to p + e^- + \bar{\nu}_e + \gamma$ was used as an auxiliary process in the analysis of the radiative corrections to the neutron β^- decay for the cancellation of infrared divergences, coming from the virtual photon exchanges [1–7]. Only starting from 1996 has it been accepted as a physical process because of the work by Gaponov and Khafizov [8], who made the first calculation of the energy spectrum and the decay rate. Then, the neutron radiative β^- decay was reinvestigated in [9] and [10,11]. The first experimental data $\mathrm{BR}_{\beta\gamma} = 3.13(35) \times 10^{-3}$ and $\mathrm{BR}_{\beta\gamma} = 3.09(32) \times 10^{-3}$, measured by Nico *et al.* [12] and Cooper *et al.* [13], for the photon-energy region $15\ \mathrm{keV} \le \omega \le 340\ \mathrm{keV}$, were in agreement within one standard deviation with the theoretical values $\mathrm{BR}_{\beta\gamma} = 2.87 \times 10^{-3}$ [10] and $\mathrm{BR}_{\beta\gamma} = 2.85 \times 10^{-3}$, calculated by Gardner [12] using the theoretical decay rate, published in [9]. Recently new precise experimental values of the branching ratios of the radiative β^- decay of a free neutron have been reported by the RDK II Collaboration Bales *et al.* [14]: $\mathrm{BR}^{(\mathrm{exp})}_{\beta\gamma} = 3.35(16) \times 10^{-3}$ and $\mathrm{BR}^{(\mathrm{exp})}_{\beta\gamma} = 5.82(66) \times 10^{-3}$, measured for the photon-energy regions $14\ \mathrm{keV} \le \omega \le 782\ \mathrm{keV}$ and $0.4\ \mathrm{keV} \le \omega \le 14\ \mathrm{keV}$, respectively. Recently [15] the rate of the neutron radiative β^- decay has been recalculated in the Standard Model (SM) and in the tree approximation to next-to-leading order in the large proton mass expansion by taking into account the contributions of the weak magnetism and proton recoil. As has been found the new theoretical values of the branching ratios $\mathrm{BR}_{\beta\gamma} = 3.04 \times 10^{-3}$ and $\mathrm{BR}_{\beta\gamma} = 5.08 \times 10^{-3}$, calculated for experimental photon-energy regions $14\ \mathrm{keV} \le \omega \le 782\ \mathrm{keV}$ and $0.4\ \mathrm{keV} \le \omega \le 14\ \mathrm{keV}$, respectively, agree with new experimental values $\mathrm{BR}^{(\mathrm{exp})}_{\beta\gamma} = 3.35(16) \times 10^{-3}$ and $\mathrm{BR}^{(\mathrm{exp})}_{\beta\gamma} = 5.82(66) \times 10^{-3}$ only within 2 and 1.2 standard deviations. As has been shown in [15] the relative contributions of the weak magnetism and proton recoil to the branching ratios of the neutron radiative β^- decay are of about 0.7%. Of course, these contributions are small compared to the error bars of the experimental values but they are by a factor 4 larger than the contribution of the weak magnetism and proton recoil 0.16% to the rate of the neutron β^- decay [10]. As has been pointed out in [15] the contributions to the rate of the neutron radiative β^- decay, calculated in the SM and in the tree approximation to next-to-leading order in the large baryon mass expansion including the contributions of baryon resonances (see, for example, Bernard *et al.* [9]), cannot in principle exceed 1.5%. So one may expect some tangible contributions only beyond the tree approximation, taking into account, for example, one-virtual-photon exchanges to leading order in the large proton mass expansion, i.e., the radiative corrections of order $O(\alpha/\pi)$. We would like to remind the reader that radiative corrections of order $O(\alpha/\pi)$ change the rate of the neutron β^- decay by about 3.75% [10,15]. Because of an enhancement of the contributions of order $1/M$, where $2M = m_n + m_p$ is an averaged nucleon mass [10,15], to the rate of the neutron radiative β^- decay, one may also expect an enhancement of the relative contributions of the radiative corrections of order $O(\alpha/\pi)$.

For the first time the radiative corrections of order $O(\alpha/\pi)$ for the analysis of T-odd momentum correlations

*ivanov@kph.tuwien.ac.at
†roman.hoellwieser@gmail.com
‡natroitskaya@yandex.ru
§max.wellenzohn@gmail.com
‖berdnikov@spbstu.ru

in the neutron radiative β^- decay to order $O(\alpha^2/\pi^2)$ have been calculated by Gardner and He [16,17]. In this paper we give a complete analysis of the radiative corrections to order $O(\alpha/\pi)$ to the rate of the neutron radiative β^- decay, caused by pure quantum electrodynamics (QED), where photons couple to the pointlike proton and electron with a contribution of strong low-energy interactions defined by the axial coupling constant λ only.

A complete set of Feynman diagrams, describing the amplitude of the neutron radiative β^- decay in the tree and one-loop approximation, are shown in Figs. 1–5. In Figs. 1–4 the states of real and virtual photons with 4-momenta k and q, respectively, are described by the polarization vector $\varepsilon^*_{\lambda'}(k)$ with $\lambda' = 1, 2$ and a Green function $D_{\alpha\beta}(q) = (\eta_{\alpha\beta} - (1-\xi)q_\alpha q_\beta/q^2)/(q^2 + i0)$ [10], where the polarization vector obeys the constraint $\varepsilon^*_{\lambda'}(k)\cdot k = 0$ with $k^2 = 0$ and ξ is a gauge parameter. The Feynman diagrams in Fig. 5 describe a neutron radiative β^- decay with two real photons in the final state. Integrating over degrees of freedom of one of the photons one obtains the contribution of order $O(\alpha^2/\pi^2)$ to the rate of the neutron radiative β^- decay with one real photon in the final state. The contributions of strong low-energy hadronic interactions in the Feynman diagrams Figs. 1–5 (see also Fig. [6]) are denoted by shaded regions.

The contributions of pure QED are given by the Feynman diagrams in Figs. 1(a), 1(b), 2, and 5, where real and virtual photons couple to the pointlike proton and electron and strong low-energy hadronic and electromagnetic interactions are factorized. The contribution of strong low-energy interactions is described by the axial coupling constant λ only. In the diagram Fig. 1(c) a real photon is emitted by a hadronic block. In spite of a possible dependence of the contribution of this diagram on electron and photon energies it has been neglected in the first calculations of the neutron radiative β^- decay by Gaponov and Khafizov [8] and in the subsequent calculations by Bernard *et al.* [9] and Ivanov *et al.* [10,15]. In this paper we also accept such an approximation. We neglect the contributions of all Feynman diagrams, where even if one photon (real or virtual) is emitted or absorbed by a hadronic block. In Sec. IV we propose a justification of the neglect of the contribution of the diagram in Fig. 1(c). However, an analysis of contributions of strong low-energy hadronic interactions in the diagrams in Figs. 3 and 4 demands a special consideration and goes beyond the scope of this paper.

It is well known that the amplitude of the neutron radiative β^- decay should be gauge invariant. This means that when making a gauge transformation of a real photon wave function, i.e., replacing the photon polarization vector $\varepsilon^*_{\lambda'}(k)$ by $\varepsilon^*_{\lambda'}(k) \to \varepsilon^*_{\lambda'}(k) + ck$, where c is an arbitrary constant, the contribution proportional to ck should vanish [18] (see also [19]). In Appendixes A and B of the Supplemental Material [20] we investigate the properties of Feynman diagrams in Figs. 1 and 2 with respect to a gauge transformation $\varepsilon^*_{\lambda'}(k) \to \varepsilon^*_{\lambda'}(k) + ck$. By means of a direct calculation we show that in Fig. 1 the sum of the diagrams Figs. 1(a) and 1(b) is gauge invariant. This implies that the diagram Fig. 1(c) should be gauge invariant

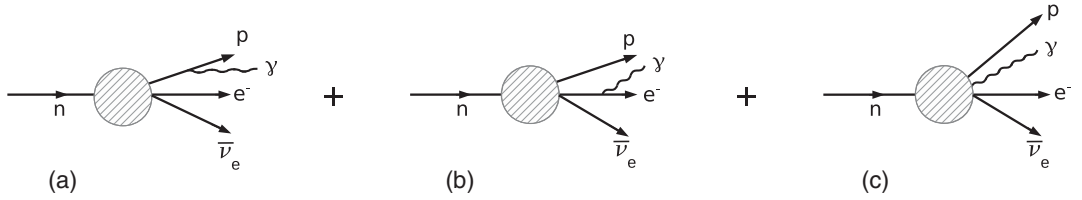

FIG. 1. The Feynman diagrams, defining the contribution to the amplitude of the neutron radiative β^- decay in the tree approximation to order e.

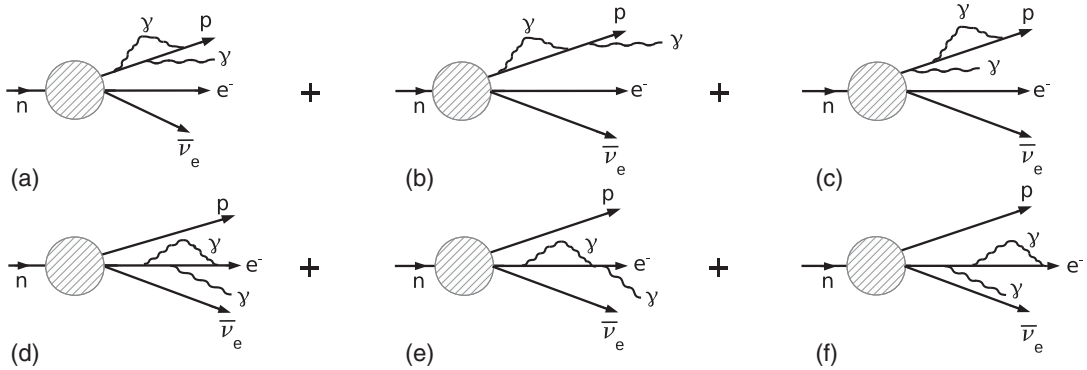

FIG. 2. The Feynman diagrams, defining the contribution to the amplitude of the neutron radiative β^- decay of order e^3, caused by pure QCD.

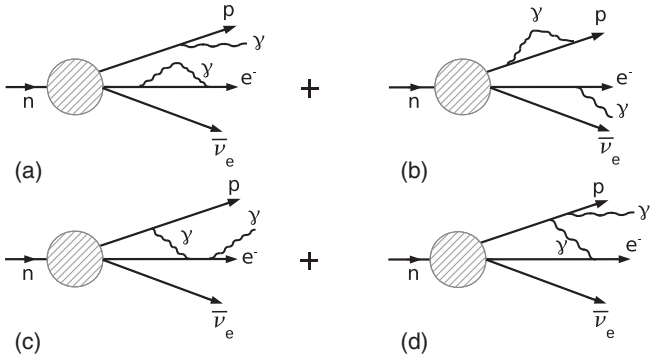

FIG. 3. The Feynman diagrams, defining the main contribution to the amplitude of the neutron radiative β^- decay of order e^3.

by itself. In turn, in Fig. 2 the diagrams with photons coupled to the proton [Figs. 2(a)–2(c)] and electron [Figs. 2(d)–2(f)] are invariant under a gauge transformation $\varepsilon^*_{\lambda'}(k) \to \varepsilon^*_{\lambda'}(k) + ck$ separately. We show that invariance of the diagrams in Fig. 2 with respect to a gauge transformation $\varepsilon^*_{\lambda'}(k) \to \varepsilon^*_{\lambda'}(k) + ck$ leads to Ward identities, which impose well-known constraints on the renormalization parameters [18] and certain constraints on the structure functions (see Appendix B of the Supplemental Material [20]). It is important to emphasize that to leading order in the large proton mass expansion the contribution of the diagram in Fig. 1(a) is proportional to the time component of the photon polarization vector $\varepsilon^{0*}_{\lambda'}(k)$, which vanishes in the physical gauge $\varepsilon^*_{\lambda'}(k) = (0, \vec{\varepsilon}^*_{\lambda'}(\vec{k}))$, where the polarization vector $\vec{\varepsilon}^*_{\lambda'}(\vec{k})$ obeys the constraint $\vec{k} \cdot \vec{\varepsilon}^*_{\lambda'}(\vec{k}) = 0$ [21] (see also [10,15,22]). As has been shown in [8–10,15] the contribution of the diagrams in Fig. 1, taken to leading order in the large proton mass expansion with a real photon in the physical gauge $\varepsilon^*_{\lambda'}(k) = (0, \vec{\varepsilon}^*_{\lambda'}(\vec{k}))$, describes well

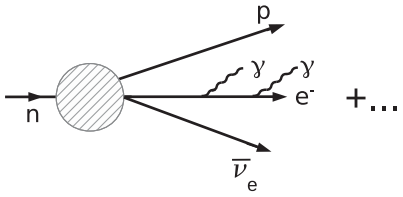

FIG. 5. The Feynman diagrams, defining the main contribution of order $O(\alpha^2/\pi^2)$ to the rate of the neutron radiative β^- decay $n \to p + e^- + \bar{\nu}_e + \gamma + \gamma$ with one detected and one undetected photon.

the main part of the branching ratio of the neutron radiative β^- decay (see Table I).

As regards the diagrams in Fig. 2, to leading order in the large proton mass expansion the contribution of the diagrams Figs. 2(a)–2(c) becomes proportional to $\varepsilon^{0*}_{\lambda'}(k)$ and vanishes in the physical gauge $\varepsilon^*_{\lambda'}(k) = (0, \vec{\varepsilon}^*_{\lambda'}(\vec{k}))$. As a result, only the diagrams Figs. 2(d)–2(f) give a contribution to the amplitude of the neutron radiative β^- decay, calculated to leading order in the large proton mass expansion with a real photon in the physical gauge $\varepsilon^*_{\lambda'}(k) = (0, \vec{\varepsilon}^*_{\lambda'}(\vec{k}))$ (see Appendix B of the Supplemental Material [20]).

According to Sirlin [5], the contributions of the Feynman diagrams with one-loop corrections, which are shown in Figs. 2–4, should be also invariant under a gauge transformation of a virtual photon, which reduces to a redefinition of a longitudinal part of a photon Green function $D_{\alpha\beta}(q) \to D_{\alpha\beta}(q) + c(q^2) q_\alpha q_\beta$, where $c(q^2)$ is an arbitrary function of q^2 [5]. In Appendix B of the Supplemental Material [20] we show that the contributions of the diagrams in Fig. 2 are invariant also under a gauge transformation $D_{\alpha\beta}(q) \to D_{\alpha\beta}(q) + c(q^2) q_\alpha q_\beta$.

Unlike the Feynman diagrams in Fig. 2 the properties and calculation of the set of Feynman diagrams in

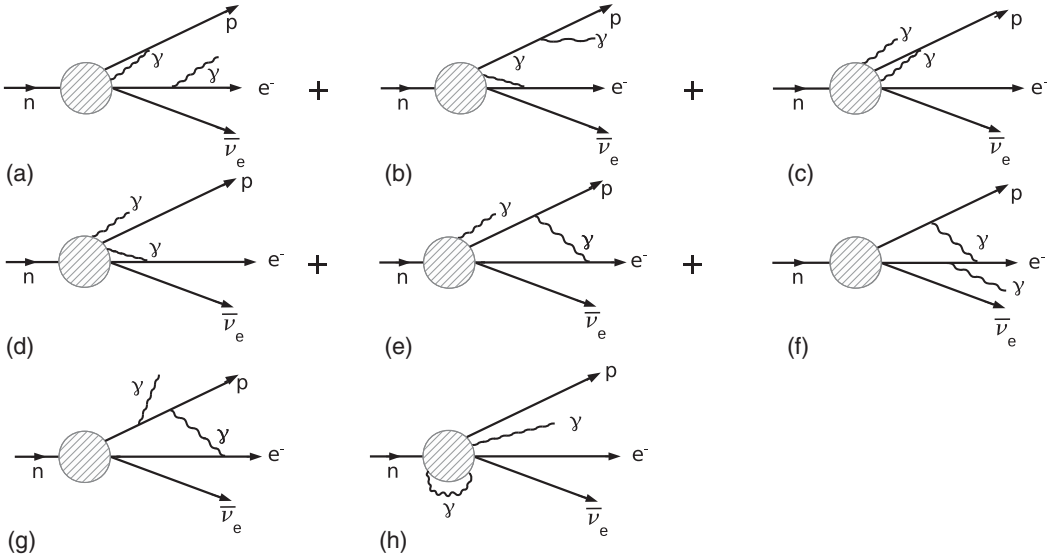

FIG. 4. The Feynman diagrams, responsible for restoration of the gauge invariance of the Feynman diagrams Figs. 3(c) and 3(d).

TABLE I. Branching ratios of the neutron radiative β^- decay for three photon-energy regions, calculated for the lifetime of the neutron $\tau_n = 879.6(1.1)$ s [10]. The branching ratio $\mathrm{BR}_{\beta\gamma}^{(\mathrm{Fig.1})}$ takes into account the contributions of the weak magnetism and proton recoil, calculated in [15] to next-to-leading order in the large proton mass expansion.

ω (keV)	$\mathrm{BR}_{\beta\gamma}$ (experiment)	$\mathrm{BR}_{\beta\gamma}^{(\mathrm{Fig.1})}$	$\mathrm{BR}_{\beta\gamma}^{(\mathrm{Fig.2})}$	$\mathrm{BR}_{\beta\gamma}^{(\mathrm{Fig.3})}$	$\mathrm{BR}_{\beta\gamma}^{(\mathrm{Fig.5})}$	$\mathrm{BR}_{\beta\gamma}$ (theory)
$15 \le \omega \le 340$	$(3.09 \pm 0.32) \times 10^{-3}$ [13]	2.89×10^{-3}	0.95×10^{-7}	0.65×10^{-4}	0.52×10^{-5}	2.960×10^{-3}
$14 \le \omega \le 782$	$(3.35 \pm 0.05[\mathrm{stat}] \pm 0.15[\mathrm{syst}]) \times 10^{-3}$ [14]	3.04×10^{-3}	1.23×10^{-7}	0.68×10^{-4}	0.55×10^{-5}	3.114×10^{-3}
$0.4 \le \omega \le 14$	$(5.82 \pm 0.23[\mathrm{stat}] \pm 0.62[\mathrm{syst}]) \times 10^{-3}$ [14]	5.08×10^{-3}	0.03×10^{-7}	1.54×10^{-4}	3.23×10^{-5}	5.266×10^{-3}

Figs. 3 and 4 are not so simple and transparent. In Appendix C of the Supplemental Material [20] we show that the contributions of the diagrams Figs. 3(a) and 3(b), where strong low-energy and electromagnetic interactions are factorized, vanish after renormalization of masses and wave functions of the proton and electron. In turn, the diagrams Figs. 3(c) and 3(d) cannot be treated separately from the diagrams in Fig. 4, since by themselves they are not invariant under gauge transformations $\varepsilon^*_{\lambda'}(k) \to \varepsilon^*_{\lambda'}(k) + ck$ and $D_{\alpha\beta}(q) \to D_{\alpha\beta}(q) + c(q^2) q_\alpha q_\beta$. Following Sirlin [5] we assume that required gauge invariance can be fulfilled only for a sum of the Feynman diagrams Figs. 3(c), 3(d), and 4, where strong low-energy hadronic and electromagnetic interactions are overlapped and photons (real and virtual) are emitted or absorbed by a hadronic block.

Such an assertion is not proved but based on the following observation. After a removal of the lines of a real photon emission the diagrams Figs. 3(c) and 3(d) reduce themselves to the diagram Fig. 6(a), which, as has been shown by Sirlin [5], gives the main contribution of the radiative corrections of order $O(\alpha/\pi)$ to the rate of the neutron β^- decay. However, the diagram Fig. 6(a) by itself is not invariant under a gauge transformation $D_{\alpha\beta}(q) \to D_{\alpha\beta}(q) + c(q^2) q_\alpha q_\beta$. As has been pointed out by Sirlin [5], only a sum of the diagrams in Fig. 6 should be gauge invariant. However, an exact calculation of the diagrams Figs. 6(b) and 6(c) demands a certain model of strong low-energy interactions of hadrons coupled to photons at low energies. Nevertheless, Sirlin, using the current algebra approach [5,23], has succeeded in showing that the contributions of the diagrams Figs. 6(b) and 6(c) do not depend on the electron energy E_e. Such a remarkable property of these diagrams has allowed Sirlin to decompose the contribution of the diagram Fig. 6(a) into invariant and noninvariant parts with respect to a gauge transformation $D_{\alpha\beta}(q) \to D_{\alpha\beta}(q) + c(q^2) q_\alpha q_\beta$ in such a way that a gauge-noninvariant part does not depend on the electron energy. Then, a constant gauge-noninvariant part has been merely absorbed by formal renormalization of the Fermi weak coupling constant G_F and the axial coupling constant λ. We would like to emphasize that, unfortunately, the diagrams Figs. 3(c) and 3(d) do not possess such a remarkable property. Nevertheless, it is obvious that different insertions of real photon lines transform the diagrams in Fig. 6 into a set of Feynman diagrams Figs. 3(c), 3(d), and 4 and should not destroy gauge invariance of these diagrams with respect to a gauge transformation $D_{\alpha\beta}(q) \to D_{\alpha\beta}(q) + c(q^2) q_\alpha q_\beta$. As a result, the analytical analysis of the diagrams Figs. 3(c), 3(d), and 4, which is performed in Appendixes C and D of the Supplemental Material [20], runs as follows. Firstly, we show that to leading order in the large proton mass expansion the diagram Fig. 3(d), calculated with the contribution of strong low-energy hadronic interactions given by the axial coupling constant λ only, vanishes in the physical gauge of a real photon $\varepsilon^*_{\lambda'}(k) = (0, \vec{\varepsilon}^{\,*}_{\lambda'}(\vec{k}))$. Secondly, we calculate the diagram Fig. 3(c) to leading order in the large proton mass expansion and in the physical gauge of a real photon. After that we decompose the contribution of the diagram Fig. 3(c) into invariant and noninvariant parts with respect to a gauge transformation $D_{\alpha\beta}(q) \to D_{\alpha\beta}(q) + c(q^2) q_\alpha q_\beta$. Keeping only the part that is invariant under a gauge transformation $D_{\alpha\beta}(q) \to D_{\alpha\beta}(q) + c(q^2) q_\alpha q_\beta$, and removing from it a part independent of the electron E_e and photon ω energy by renormalization of the Fermi weak coupling and axial coupling constant, we obtain a contribution, which can be accepted as a physical contribution of the diagram Fig. 3(c) to the amplitude and rate of the

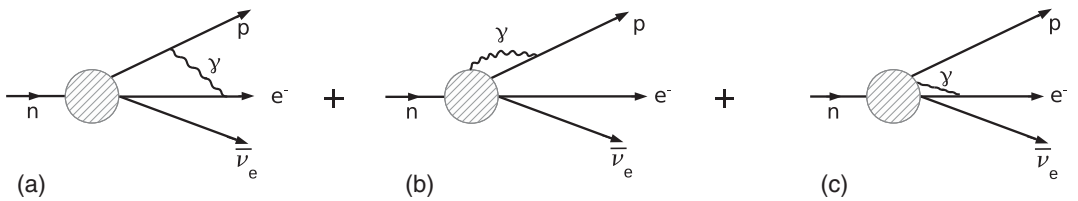

FIG. 6. The Feynman diagrams, defining the main contribution of the radiative corrections of order $O(\alpha/\pi)$, caused by one-virtual-photon exchanges, to the neutron β^- decay (see Sirlin [5]).

neutron radiative β^- decay to order $O(\alpha^2/\pi^2)$. What then is the role of the Feynman diagrams in Fig. 4?

As regards the diagrams in Fig. 4, since the contribution of them cannot be calculated in a model-independent way, we follow Sirlin [5] and assume that the diagrams in Fig. 4 (i) cancel a gauge-noninvariant part of the diagram Fig. 3(c), determined relative to a gauge transformation $D_{\alpha\beta}(q) \to D_{\alpha\beta}(q) + c(q^2)q_\alpha q_\beta$, and the rest (ii) either vanishes to leading order in the proton mass expansion in the physical gauge of a real photon $\varepsilon^*_{\lambda'}(k) = (0, \vec{\varepsilon}^{\,*}_{\lambda'}(\vec{k}))$ (see Appendix D of the Supplemental Material [20]) or (iii) is a constant, which can be absorbed by renormalization of the Fermi coupling constant G_F and the axial coupling constant λ. This agrees also well with an assumption that different insertions of real photons' lines into the diagrams in Fig. 6 do not corrupt the properties of the Feynman diagrams in Figs. 3(c), 3(d), and 4 under a gauge transformation of a photon Green function $D_{\alpha\beta}(q) \to D_{\alpha\beta}(q) + c(q^2)q_\alpha q_\beta$ even if to leading order in the large proton mass expansion. In Appendix D of the Supplemental Material [20] we analyze the contributions of the diagrams Figs. 4(f) and 4(g), where strong low-energy interactions are given by the axial coupling constant λ only. We show that to leading order in the large proton mass expansion the contributions of these diagrams vanish. Hence, an important contribution, which may cancel a gauge-noninvariant part of the diagram Fig. 3(c), is able to come only from the diagrams, where a real or virtual photon couple to a hadronic block.

The diagram in Fig. 5 defines one of a set of Feynman diagrams of the neutron radiative β^- decay with emission of two real photons. Such a process with one undetected photon can imitate a contribution of order $O(\alpha^2/\pi^2)$ to the rate of the neutron radiative β^- decay. All diagrams of the neutron radiative β^- decay with emission of one or two photons by the proton, calculated to leading order in the large proton mass expansion, do not contribute to the rate of the neutron radiative β^- decay in the physical gauge of real photons. Then, the contributions of the diagrams with emission of photons from the hadronic blocks are neglected (see a discussion in Sec. IV). Thus, in the accepted approximation the main contribution to the rate of the neutron radiative β^- decay is defined by the Feynman diagrams in Fig. 5 with the account for the contributions, caused by symmetry of the final state with respect to symmetry properties of the two photons in the final state of the decay. For the analytical calculation of the diagram in Fig. 5 the contribution of strong low-energy interactions is defined by the axial coupling only. The analytical calculation of the diagrams in Fig. 5 is given in Appendix E of the Supplemental Material [20].

The paper is organized as follows. In Sec. II we give a short description of the renormalization procedure of effective low-energy electroweak interactions for the neutron radiative β^- decay. In Sec. III we adduce the contributions of the Feynman diagrams in Figs. 1–5 to the rate of the neutron radiative β^- decay. The numerical values of the branching ratio of the neutron radiative β^- decay for the three regions of photon energies (i) $15\ \text{keV} \le \omega \le 350\ \text{keV}$, (ii) $14\ \text{keV} \le \omega \le 782\ \text{keV}$ and (iii) $0.4\ \text{keV} \le \omega \le 14\ \text{keV}$ are given in Table I. In Sec. IV we discuss the obtained results. In the Supplemental Material [20] we give detailed analytical calculations and analysis of the contributions of Feynman diagrams in Figs. 1–5 to the amplitude and rate of the neutron radiative β^- decay.

Of course, we have to confess that the main problem of our analysis of the radiative corrections to order $O(\alpha/\pi)$, defining corrections to order $O(\alpha^2/\pi^2)$ to the rate of the neutron radiative β^- decay, concerns the contributions of diagrams with real or virtual photons coupled to a hadronic block. A justification of our assumption concerning the properties of these diagrams within a certain model of strong low-energy interactions of hadrons coupled to photons should be important for a confirmation of the approximation accepted in this paper and the results obtained therein. We would like to accentuate that unlike a passive role of strong low-energy hadronic interactions in the radiative corrections of order $O(\alpha/\pi)$ to the rate of the neutron β^- decay, strong low-energy interactions of hadrons coupled to real and virtual photons in the diagrams in Fig. 4 should play a more important role, going beyond a formal renormalization of the Fermi weak coupling and axial coupling constant, but give some contributions, which depend on the electron and photon energies and momenta, and should cancel a gauge-noninvariant part of the diagram Fig. 3(c). The observed peculiarities of the Feynman diagrams Figs. 3 and 4 agree well with an important role of strong low-energy hadronic interactions in decay processes that have been already pointed out by Weinberg [24]. Thus, the problem of strong low-energy hadronic interactions in the neutron radiative β^- decay to order $O(\alpha^2/\pi^2)$ demands a special analysis and we are planning to perform such a model-dependent analysis of the neutron radiative β^- decay to order $O(\alpha^2/\pi^2)$ in our forthcoming publication.

II. RENORMALIZATION PROCEDURE OF EFFECTIVE LOW-ENERGY ELECTROWEAK INTERACTIONS FOR THE NEUTRON RADIATIVE β^- DECAY

In the Standard Model of electroweak interactions the neutron radiative β^- decay, defined in the one-loop approximation with one-virtual-photon exchanges, is described by the following interactions,

$$\mathcal{L}_{\rm int}(x) = \mathcal{L}_{\rm W}(x) + \mathcal{L}_{\rm em}(x), \tag{1}$$

where $\mathcal{L}_{\rm W}(x)$ is the effective Lagrangian of low-energy $V-A$ interactions with a real axial coupling constant $\lambda = -1.2750(9)$ [25] (see also [10,15]),

$$\mathcal{L}_{\rm W}(x) = -\frac{G_F}{\sqrt{2}} V_{ud}[\bar{\psi}_p(x)\gamma_\mu(1+\lambda\gamma^5)\psi_n(x)] \times [\bar{\psi}_e(x)\gamma^\mu(1-\gamma^5)\psi_\nu(x)], \quad (2)$$

where $G_F = 1.1664 \times 10^{-11}$ MeV^{-2} is the Fermi coupling constant, and $|V_{ud}| = 0.97417(21)$ is the Cabibbo-Kobayashi-Maskawa matrix element [26]. Then, $\psi_p(x)$, $\psi_n(x)$, $\psi_e(x)$ and $\psi_\nu(x)$ are the field operators of the proton, neutron, electron and antineutrino, respectively, and γ^μ and γ^5 are the Dirac matrices [18]. Since we calculate the radiative corrections of order $O(\alpha/\pi)$ to the neutron radiative β^- decay to leading order in the large proton mass expansion, in the effective Lagrangian $\mathcal{L}_{\rm W}(x)$ we do not take into account the contribution of the weak magnetism proportional to $1/M$, where $2M = m_n + m_p$ is an averaged nucleon mass [15].

For the calculation of the radiative corrections to order $O(\alpha/\pi)$ of the Lagrangian of the electromagnetic interaction $\mathcal{L}_{\rm em}(x)$ we take in the following form,

$$\begin{aligned}\mathcal{L}_{\rm em}(x) =& -\frac{1}{4}F^{(0)}_{\mu\nu}(x)F^{(0)\mu\nu}(x) - \frac{1}{2\xi_0}(\partial_\mu A^{(0)\mu}(x))^2 \\ &+ \bar{\psi}_{0e}(x)(i\gamma^\mu\partial_\mu - m_{0e})\psi_{0e}(x) \\ &- (-e_0)\bar{\psi}_{0e}(x)\gamma^\mu\psi_{0e}(x)A^{(0)}_\mu(x) \\ &+ \bar{\psi}_{0p}(x)(i\gamma^\mu\partial_\mu - m_{0p})\psi_{0p}(x) \\ &- (+e_0)\bar{\psi}_{0p}(x)\gamma^\mu\psi_{0p}(x)A^{(0)}_\mu(x), \end{aligned} \quad (3)$$

where $F^{(0)}_{\mu\nu}(x) = \partial_\mu A^{(0)}_\nu(x) - \partial_\nu A^{(0)}_\mu(x)$ is the electromagnetic field strength tensor of the bare (unrenormalized) electromagnetic field operator $A^{(0)}_\mu(x)$; $\psi_{0e}(x)$ and $\psi_{0p}(x)$ are bare operators of the electron and proton fields with bare masses m_{0e} and m_{0p}, respectively; and $-e_0$ and $+e_0$ are bare electric charges of the electron and proton, respectively. Then, ξ_0 is a bare gauge parameter. After the calculation of the one-loop corrections of order $O(\alpha/\pi)$ a transition to the renormalized field operators, masses and electric charges is defined by the Lagrangian

$$\begin{aligned}\mathcal{L}_{\rm em}(x) =& -\frac{1}{4}F_{\mu\nu}(x)F^{\mu\nu}(x) - \frac{1}{2\xi}(\partial_\mu A^\mu(x))^2 \\ &+ \bar{\psi}_e(x)(i\gamma^\mu\partial_\mu - m_e)\psi_e(x) \\ &- (-e)\bar{\psi}_e(x)\gamma^\mu\psi_e(x)A_\mu(x) \\ &+ \bar{\psi}_p(x)(i\gamma^\mu\partial_\mu - m_p)\psi_p(x) \\ &- (+e)\bar{\psi}_p(x)\gamma^\mu\psi_p(x)A_\mu(x) + \delta\mathcal{L}_{\rm em}(x), \end{aligned} \quad (4)$$

where $A_\mu(x)$, $\psi_e(x)$ and $\phi_p(x)$ are the renormalized operators of the electromagnetic, electron and proton fields, respectively; m_e and m_p are the renormalized masses of the electron and proton; e is the renormalized electric charge; and ξ is the renormalized gauge parameter. The Lagrangian $\delta\mathcal{L}_{\rm em}(x)$ contains a complete set of the counterterms [27],

$$\begin{aligned}\delta\mathcal{L}_{\rm em}(x) =& -\frac{1}{4}(Z_3-1)F_{\mu\nu}(x)F^{\mu\nu}(x) - \frac{Z_3-1}{Z_\xi}\frac{1}{2\xi}(\partial_\mu A^\mu(x))^2 \\ &+ (Z^{(e)}_2-1)\bar{\psi}_e(x)(i\gamma^\mu\partial_\mu - m_e)\psi_e(x) \\ &- (Z^{(e)}_1-1)(-e)\bar{\psi}_e(x)\gamma^\mu\psi_e(x)A_\mu(x) \\ &- Z^{(e)}_2\delta m_e\bar{\psi}_e(x)\psi_e(x) \\ &+ (Z^{(p)}_2-1)\bar{\psi}_p(x)(i\gamma^\mu\partial_\mu - m_p)\psi_p(x) \\ &- (Z^{(p)}_1-1)(+e)\bar{\psi}_p(x)\gamma^\mu\psi_p(x)A_\mu(x) \\ &- Z^{(p)}_2\delta m_p\bar{\psi}_p(x)\psi_p(x), \end{aligned} \quad (5)$$

where Z_3, $Z^{(e)}_2$, $Z^{(e)}_1$, $Z^{(p)}_2$, $Z^{(p)}_1$, δm_e and δm_p are the counterterms. Here Z_3 is the renormalization constant of the electromagnetic field operator A_μ, $Z^{(e)}_2$ and $Z^{(e)}_1$ are the renormalization constants of the electron field operator ψ_e and the electron-electron-photon $(e^-e^-\gamma)$ vertex, respectively; $Z^{(p)}_2$ and $Z^{(p)}_1$ are the renormalization constants of the proton field operator ψ_p and the proton-proton-photon $(pp\gamma)$ vertex, respectively. Then, $(-e)$ and $(+e)$, m_e and m_p, and δm_e and δm_p are the renormalized electric charges and masses and the mass counterterms of the electron and proton, respectively. Rescaling the field operators [27,28]

$$\begin{aligned}\sqrt{Z_3}A_\mu(x) &= A^{(0)}_\mu(x), \\ \sqrt{Z^{(e)}_2}\psi_e(x) &= \psi_{0e}(x), \\ \sqrt{Z^{(p)}_2}\psi_p(x) &= \psi_{0p}(x) \end{aligned} \quad (6)$$

and denoting $m_e + \delta m_e = m_{0e}$, $m_p + \delta m_p = m_{0p}$ and $Z_\xi\xi = \xi_0$ we arrive at the Lagrangian

$$\begin{aligned}\mathcal{L}_{\rm em}(x) =& -\frac{1}{4}F^{(0)}_{\mu\nu}(x)F^{(0)\mu\nu}(x) - \frac{1}{2\xi_0}(\partial_\mu A^{(0)\mu}(x))^2 \\ &+ \bar{\psi}_{0e}(x)(i\gamma^\mu\partial_\mu - m_{0e})\psi_{0e}(x) \\ &- (-e)Z^{(e)}_1(Z^{(e)}_2)^{-1}Z_3^{-1/2}\bar{\psi}_{0e}(x)\gamma^\mu\psi_{0e}(x)A^{(0)}_\mu(x) \\ &+ \bar{\psi}_{0p}(x)(i\gamma^\mu\partial_\mu - m_{0p})\psi_{0p}(x) \\ &- (+e)Z^{(p)}_1(Z^{(p)}_2)^{-1}Z_3^{-1/2}\bar{\psi}_{0p}(x)\gamma^\mu\psi_{0p}(x)A^{(0)}_\mu(x). \end{aligned} \quad (7)$$

Because of the Ward identities $Z^{(e)}_1 = Z^{(e)}_2$ and $Z^{(p)}_1 = Z^{(p)}_2$ [18,27,28], we may replace $(-e)Z_3^{-1/2} = -e_0$ and $(+e)Z_3^{-1/2} = +e_0$. This brings Eq. (7) to the form of Eq. (3). We would like to emphasize that to order $O(\alpha/\pi)$ the renormalization constant Z_3 is equal to unity, i.e., $Z_3 = 1$. This is because of the absence of closed fermion loops, giving contributions of order $O(\alpha^2/\pi^2)$ to the amplitude of the neutron radiative β^- decay that goes

beyond the accepted approximation $O(\alpha/\pi)$ for the amplitude and $O(\alpha^2/\pi^2)$ for the rate of the neutron radiative β^- decay. Hence, to order $O(\alpha/\pi)$ the bare e_0 and renormalized e electric charges are equal, i.e., $e_0 = e$. Now we may proceed to the discussion of the contributions of the radiative corrections of order $O(\alpha/\pi)$, where $\alpha = e^2/4\pi = 1/137.036$ is the fine-structure constant [26], to the amplitude and rate of the neutron radiative β^- decay. The detailed calculations and analysis of the Feynman diagrams in Figs. 2–5, defining a complete set of radiative corrections of order $O(\alpha/\pi)$, we give in the Supplemental Material [20]. In Sec. III we adduce the analytical expressions for the contributions of the diagrams in Figs. 2–5 to the rate of the neutron radiative β^- decay. The numerical values are collected in Table I. For completeness we take into account the tree-level contribution, given by the Feynman diagrams in Fig. 1 and calculated in [15] to order $1/M$, including corrections of the weak magnetism and proton recoil.

III. RATE OF NEUTRON RADIATIVE β^- DECAY WITH ONE DETECTED PHOTON

The rate of the neutron radiative β^- decay with a photon, detected in the photon-energy region $\omega_{\rm min} \le \omega \le \omega_{\rm max}$, is given by

$$\lambda_{\beta\gamma}(\omega_{\rm max},\omega_{\rm min}) = \sum_{j=1}^{5} \lambda_{\beta\gamma}^{(\rm Fig\,j)}(\omega_{\rm max},\omega_{\rm min}), \tag{8}$$

where $\lambda_{\beta\gamma}^{(\rm Fig\,j)}(\omega_{\rm max},\omega_{\rm min})$ are the rates, caused by the contributions of the diagrams in Fig. j for $j = 1, 2, \ldots, 5$. They are calculated in the Supplemental Material [20]. To leading order in the large proton mass expansion the contribution of the diagrams in Fig. 1 is equal to [10]

$$\lambda_{\beta\gamma}^{(\rm Fig.1)}(\omega_{\rm max},\omega_{\rm min}) = (1+3\lambda^2)\frac{\alpha}{\pi}\frac{G_F^2|V_{ud}|^2}{2\pi^3}\int_{\omega_{\rm min}}^{\omega_{\rm max}}\frac{d\omega}{\omega}\int_{m_e}^{E_0-\omega} dE_e\sqrt{E_e^2-m_e^2}E_e F(E_e,Z=1)(E_0-E_e-\omega)^2$$
$$\times\left\{\left(1+\frac{\omega}{E_e}+\frac{1}{2}\frac{\omega^2}{E_e^2}\right)\left[\frac{1}{\beta}\ell n\left(\frac{1+\beta}{1-\beta}\right)-2\right]+\frac{\omega^2}{E_e^2}\right\}, \tag{9}$$

where $E_0 = (m_n^2 - m_p^2 + m_e^2)/2m_n$ is the end-point energy of the electron energy spectrum of the neutron β^- decay [10]; ω is a photon energy; $\beta = k_e/E_e = \sqrt{E_e^2-m_e^2}/E_e$ is a velocity of the electron with a momentum k_e; and $F(E_e, Z=1)$ is the relativistic Fermi function, describing the Coulomb proton-electron interaction in the final state of the decay. It is equal to

$$F(E_e,Z=1) = \left(1+\frac{1}{2}\gamma\right)\frac{4(2r_p m_e\beta)^{2\gamma}}{\Gamma^2(3+2\gamma)}\frac{e^{\pi\alpha/\beta}}{(1-\beta^2)^{\gamma}}\left|\Gamma\left(1+\gamma+i\frac{\alpha}{\beta}\right)\right|^2, \tag{10}$$

where $\gamma = \sqrt{1-\alpha^2}-1$, r_p is the electric radius of the proton and $\alpha = 1/137.036$ is the fine-structure constant. In numerical calculations we shall use $r_p = 0.841$ fm [29]. The rate of the neutron radiative β^- decay, calculated to next-to-leading order in the large proton mass expansion, taking into account the contributions of the weak magnetism and proton recoil to order $1/M$, where $2M = m_n + m_p$ is the averaged nucleon mass, has been calculated in [15]. The result is

$$\lambda_{\beta\gamma}^{(\rm Fig.1)}(\omega_{\rm max},\omega_{\rm min}) = (1+3\lambda^2)\frac{\alpha}{\pi}\frac{G_F^2|V_{ud}|^2}{2\pi^3}\int_{\omega_{\rm min}}^{\omega_{\rm max}}\frac{d\omega}{\omega}\int_{m_e}^{E_0-\omega} dE_e E_e\sqrt{E_e^2-m_e^2}(E_0-E_e-\omega)^2$$
$$\times F(E_e,Z=1)\rho_{\beta\gamma}^{(\rm Fig.1)}(E_e,\omega). \tag{11}$$

The function $\rho_{\beta\gamma}^{(\rm Fig.1)}(E_e,\omega)$ is given by the integral [15]

$$\rho_{\beta\gamma}^{(\rm Fig.1)}(E_e,\omega) = \int\frac{d\Omega_{e\gamma}}{4\pi}\left\{\left[1+2\frac{\omega}{M}\frac{E_e-\vec{k}_e\cdot\vec{n}_{\vec{k}}}{E_0-E_e-\omega}+\frac{3}{M}\left(E_e+\omega-\frac{1}{3}E_0\right)+\frac{\lambda^2-2(\kappa+1)\lambda+1}{1+3\lambda^2}\frac{E_0-E_e-\omega}{M}\right]\right.$$
$$\times\left[\left(1+\frac{\omega}{E_e}\right)\frac{k_e^2-(\vec{k}_e\cdot\vec{n}_{\vec{k}})^2}{(E_e-\vec{k}_e\cdot\vec{n}_{\vec{k}})^2}+\frac{\omega^2}{E_e}\frac{1}{E_e-\vec{k}_e\cdot\vec{n}_{\vec{k}}}\right]+\frac{3\lambda^2-1}{1+3\lambda^2}\frac{1}{M}\left(\frac{k_e^2+\omega\vec{k}_e\cdot\vec{n}_{\vec{k}}}{E_e}\left[\frac{k_e^2-(\vec{k}_e\cdot\vec{n}_{\vec{k}})^2}{(E_e-\vec{k}_e\cdot\vec{n}_{\vec{k}})^2}+\frac{\omega}{E_e-\vec{k}_e\cdot\vec{n}_{\vec{k}}}\right]\right.$$
$$\left.+(\omega+\vec{k}_e\cdot\vec{n}_{\vec{k}})\left[\left(1+\frac{\omega}{E_e}\right)\frac{\omega}{E_e-\vec{k}_e\cdot\vec{n}_{\vec{k}}}-\frac{m_e^2}{E_e}\frac{\omega}{(E_e-\vec{k}_e\cdot\vec{n}_{\vec{k}})^2}\right]\right)-\frac{\lambda^2+2(\kappa+1)\lambda-1}{1+3\lambda^2}\frac{1}{M}\left[\frac{k_e^2+\omega^2+2\omega\vec{k}_e\cdot\vec{n}_{\vec{k}}}{E_e}\right.$$
$$\left.\left.\times\frac{k_e^2-(\vec{k}_e\cdot\vec{n}_{\vec{k}})^2}{(E_e-\vec{k}_e\cdot\vec{n}_{\vec{k}})^2}+\frac{\omega}{E_e}\frac{k_e^2-(\vec{k}_e\cdot\vec{n}_{\vec{k}})^2}{E_e-\vec{k}_e\cdot\vec{n}_{\vec{k}}}+\frac{\omega^2}{E_e}\frac{\omega+\vec{k}_e\cdot\vec{n}_{\vec{k}}}{E_e-\vec{k}_e\cdot\vec{n}_{\vec{k}}}\right]-\frac{\lambda(\lambda-1)}{1+3\lambda^2}\frac{1}{M}\left[\frac{\omega}{E_e}\frac{k_e^2-(\vec{k}_e\cdot\vec{n}_{\vec{k}})^2}{E_e-\vec{k}_e\cdot\vec{n}_{\vec{k}}}+3\frac{\omega^2}{E_e}\right]\right\}, \tag{12}$$

where $\kappa = \kappa_p - \kappa_n = 3.70589$ is the isovector anomalous magnetic moment of the nucleon [10,15], $d\Omega_{e\gamma}$ is an infinitesimal solid angle of the electron-photon momentum correlations $\vec{k}_e \cdot \vec{n}_{\vec{k}} = k_e \cos\theta_{e\gamma}$ and $\vec{n}_{\vec{k}} = \vec{k}/\omega$ is a unit vector along the photon 3-momentum [10,11,15]. The contribution of the diagrams in Fig. 2 is equal to (see Appendix B of the Supplemental Material [20])

$$\lambda^{(\mathrm{Fig.2})}_{\beta\gamma}(\omega_{\max},\omega_{\min}) = (1+3\lambda^2)\frac{\alpha^2}{\pi^2}\frac{G_F^2|V_{ud}|^2}{4\pi^3}\int_{\omega_{\min}}^{\omega_{\max}} d\omega \int_{m_e}^{E_0-\omega} dE_e (E_0 - E_e - \omega)^2\sqrt{E_e^2 - m_e^2}$$
$$\times F(E_e, Z=1)\int\frac{d\Omega_{e\gamma}}{4\pi}\left\{\frac{k_e^2 - (\vec{k}_e\cdot\vec{n}_{\vec{k}})^2}{(E_e - \vec{k}_e\cdot\vec{n}_{\vec{k}})^2}\mathrm{Re}F_4 + \frac{\omega}{E_e - \vec{k}_e\cdot\vec{n}_{\vec{k}}}\mathrm{Re}(2F_2 - F_3 - 2F_4)\right\}, \quad (13)$$

where F_2, F_3 and F_4 are given in Eq. (B-71) of the Supplemental Material [20] as functions of $k_e\cdot k = \omega(E_e - \vec{k}_e\cdot\vec{n}_{\vec{k}})$. The contribution of the diagrams in Figs. 3 and 4 we define as (see Appendix C of the Supplemental Material [20])

$$\lambda^{(\mathrm{Fig.3})}_{\beta\gamma}(\omega_{\max},\omega) = (1+3\lambda^2)\frac{\alpha^2}{\pi^2}\frac{G_F^2|V_{ud}|^2}{4\pi^3}\int_{\omega_{\min}}^{\omega_{\max}}\frac{d\omega}{\omega}\int_{m_e}^{E_0-\omega} dE_e F(E_e, Z=1)(E_0 - E_e - \omega)^2\sqrt{E_e^2 - m_e^2}$$
$$\times\int\frac{d\Omega_{e\gamma}}{4\pi}\left\{f_1(E_e,\vec{k}_e,\omega,\vec{k})\left[(E_e+\omega)\frac{k_e^2 - (\vec{k}_e\cdot\vec{n}_{\vec{k}})^2}{(E_e - \vec{k}_e\cdot\vec{n}_{\vec{k}})^2} + \frac{\omega^2}{E_e - \vec{k}_e\cdot\vec{n}_{\vec{k}}}\right] + f_2(E_e,\vec{k}_e,\omega,\vec{k})\left[(2(E_e+\omega)^2 - m_e^2\right.\right.$$
$$\left.\left. - \omega(E_e - \vec{k}_e\cdot\vec{n}_{\vec{k}}))\frac{k_e^2 - (\vec{k}_e\cdot\vec{n}_{\vec{k}})^2}{(E_e - \vec{k}_e\cdot\vec{n}_{\vec{k}})^2} + 2(E_e+\omega)\frac{\omega^2}{E_e - \vec{k}_e\cdot\vec{n}_{\vec{k}}} - \omega^2\right]\right\}, \quad (14)$$

where the functions $f_1(E_e,\vec{k}_e,\omega,\vec{k})$ and $f_2(E_e,\vec{k}_e,\omega,\vec{k})$ are given in Eq. (C-33) of the Supplemental Material [20]. They are defined by the contribution of the diagram Fig. 3(c), since to leading order in the large proton mass expansion and in the physical gauge of a real photon the contribution of the diagram in Fig. 3(d) vanishes. Then, the rate $\lambda^{(\mathrm{Fig.3})}_{\beta\gamma}(\omega_{\max},\omega_{\min})$ is defined by a part of the diagram Fig. 3(c), which is invariant under a gauge transformation $D_{\alpha\beta}(q) \to D_{\alpha\beta}(q) + c(q^2)q_\alpha q_\beta$. A noninvariant part of the diagram Fig. 3(c) is absorbed by the diagrams in Fig. 4. We assume that the contribution of the diagrams in Fig. 4, calculated to leading order in the large proton mass expansion and in the physical gauge of a real photon, contains only (i) an electron-photon-energy-dependent part, canceling a part of the diagram Fig. 3(c) that is noninvariant under the gauge transformation $D_{\alpha\beta}(q) \to D_{\alpha\beta}(q) + c(q^2)q_\alpha q_\beta$, and (ii) a constant, which can be absorbed by renormalization of the Fermi weak coupling constant G_F and the axial coupling constant λ similar to Sirlin's analysis of the radiative corrections to the rate of the neutron β^- decay [5]. Of course, our assumption is much stronger than Sirlin's one. Nevertheless, we believe that it is correct and it might be confirmed by a model-dependent way within a model of strong interactions of hadrons coupled to photons at low energies (see a discussion in Sec. IV).

The contribution of the diagrams in Fig. 5 of the neutron radiative β^- decay with two real photons and only one detected photon is equal to (see Appendix E of the Supplemental Material [20])

$$\lambda^{(\mathrm{Fig.5})}_{\beta\gamma}(\omega_{\max},\omega_{\min}) = (1+3\lambda^2)\frac{\alpha^2}{\pi^2}\frac{G_F^2|V_{ud}|^2}{16\pi^3}\int_{\omega_{\min}}^{\omega_{\max}} d\omega\int_{m_e}^{E_0-\omega} dE_e\sqrt{E_e^2 - m_e^2}\int_0^{E_0-E_e-\omega} dq_0 (E_0 - E_e - \omega - q_0)^2$$
$$\times F(E_e, Z=1)\int\frac{d\Omega_{e\gamma}}{4\pi}\int\frac{d\Omega_{e\gamma'}}{4\pi}(\rho^{(1)}_{e\gamma\gamma'}(E_e,\vec{k}_e,\omega,\vec{n}_{\vec{k}},q_0,\vec{n}_{\vec{q}}) + \rho^{(2)}_{e\gamma\gamma'}(E_e,\vec{k}_e,\omega,\vec{n}_{\vec{k}},q_0,\vec{n}_{\vec{q}})$$
$$+ \rho^{(2)}_{e\gamma\gamma'}(E_e,\vec{k}_e,q_0,\vec{n}_{\vec{q}},\omega,\vec{n}_{\vec{k}})), \quad (15)$$

where q_0 is the energy of an undetected photon and $\vec{n}_{\vec{q}} = \vec{q}/q_0$ is a unit vector along its 3-momentum $\vec{q}$. The functions $\rho^{(1)}_{e\gamma\gamma'}(E_e,\vec{k}_e,\omega,\vec{n}_{\vec{k}},q_0,\vec{n}_{\vec{q}})$; $\rho^{(2)}_{e\gamma\gamma'}(E_e,\vec{k}_e,\omega,\vec{n}_{\vec{k}},q_0,\vec{n}_{\vec{q}})$; and $\rho^{(2)}_{e\gamma\gamma'}(E_e,\vec{k}_e,q_0,\vec{n}_{\vec{q}},\omega,\vec{n}_{\vec{k}})$ are given by Eqs. (E-14), (E-15) and (E-16) in the Supplemental Material [20].

The numerical values of the branching ratios $\mathrm{BR}^{(\mathrm{Fig.j})}_{\beta\gamma} = \tau_n\lambda_{\beta\gamma}(\omega_{\max},\omega_{\min})_{\mathrm{Fig\,j}}$ for $j = 1, 2, \ldots, 5$ and their total contribution are given in Table I for the three photon-energy regions (i) 15 keV $\le \omega \le$ 340 keV, (ii) 14 keV $\le \omega \le$ 782 keV and

(iii) 0.4 keV $\leq \omega \leq$ 14 keV. The branching ratios $\mathrm{BR}_{\beta\gamma}^{(\mathrm{Fig.j})}$ are obtained relative to the neutron lifetime $\tau_n = 879.6(1.1)$ s, calculated in [10] and agreeing well with the world-averaged value $\tau_n = 880.2(1.0)$ s [26].

IV. CONCLUSION

We have proposed a precision analysis of the rate of the neutron radiative β^- decay $n \to p + e^- + \bar{\nu}_e + \gamma$ to order $O(\alpha^2/\pi^2)$, defined by the $1/M$ corrections, caused by the weak magnetism and proton recoil [15], and radiative corrections of order $O(\alpha/\pi)$ in the one-virtual-photon approximation, and the contribution of the neutron radiative β^- decay with two real photons $n \to p + e^- + \bar{\nu}_e + \gamma + \gamma$. Integrating over degrees of freedom of one of two photons one arrives at the contribution of order $O(\alpha^2/\pi^2)$ to the rate of the neutron radiative β^- decay $n \to p + e^- + \bar{\nu}_e + \gamma$. The contributions of the one-virtual-photon exchanges we have classified by the Feynman diagrams in Figs. 2, 3 and 4. In the diagrams in Fig. 2 the contributions of strong low-energy and electromagnetic interactions are factorized, and both the real and virtual photons couple to the pointlike proton and electron. The contribution of strong low-energy interactions of hadrons is given by the axial coupling constant λ only. All divergences, caused by virtual photon exchanges, are absorbed by renormalization of masses and wave functions of the proton and electron, the proton-proton-photon $(pp\gamma)$ and electron-electron-photon $(e^-e^-\gamma)$ vertices. Therewith, the counterterms of renormalization of the wave functions and vertices obey standard Ward identities [18,27,28]. The diagrams in Fig. 2 are invariant under gauge transformations $\varepsilon^*_{\lambda'}(k) \to \varepsilon^*_{\lambda'}(k) + ck$ of a real photon wave function and $D_{\alpha\beta}(q) \to D_{\alpha\beta}(q) + c(q^2)q_\alpha q_\beta$ of a photon Green function, respectively. The structure functions, defining the renormalized contribution of the Feynman diagrams in Fig. 2 to the amplitude of the neutron radiative β^- decay of order $O(\alpha/\pi)$, obey Ward identities. The contribution of the Feynman diagrams in Fig. 2 to the branching ratio is of order 10^{-7} (see Table I).

The dominant but most problematic contribution comes from the Feynman diagrams in Figs. 3 and 4. For the calculation of the contribution of these diagrams we follow Sirlin's assumption for the calculation of the radiative corrections of order $O(\alpha/\pi)$ to the rate of the neutron β^- decay [5]. This means that we assume that the contribution of the diagrams in Fig. 4, which survives to leading order in the large proton mass expansion in the physical gauge of a real photon, contains (i) a part of the diagram Fig. 3(c), which is not invariant under gauge transformations of a real photon wave function $\varepsilon^*_{\lambda'}(k) \to \varepsilon^*_{\lambda'}(k) + ck$ and of a photon Green function $D_{\alpha\beta}(q) \to D_{\alpha\beta}(q) + c(q^2)q_\alpha q_\beta$, respectively, and (ii) a part independent of the electron and photon energies, which can be absorbed by renormalization of the Fermi weak coupling constant G_F and the axial coupling constant λ. This is, of course, an extended interpretation of Sirlin's assumption, since in the neutron β^- decay the Feynman diagrams similar to the diagrams in Fig. 4 [see Figs. 6(b) and 6(c)] have been found independent of the electron energy, the contribution of which has been absorbed by renormalization of the Fermi weak and axial coupling constants. A confirmation of our assumption, concerning the properties of the Feynman diagrams in Figs. 3 and 4, might be supported by the fact that all possible insertions of real photon external lines transform the Feynman diagrams in Fig. 6 to the Feynman diagrams Figs. 3(c), 3(d) and 4. It is obvious that all possible insertions of real photon external lines should not change the properties of the diagrams with respect to a gauge transformation $D_{\alpha\beta}(q) \to D_{\alpha\beta} + c(q^2)q_\alpha q_\beta$. Hence, all diagrams in Fig. 4 should play an auxiliary role for the diagram Fig. 3(c) to leading order in the large proton mass expansion. Thus, such an extended Sirlin's assumption, applied to the calculation of the Feynman diagrams in Figs. 3(c), 3(d) and 4, we have realized as follows. Firstly, we have shown that in Fig. 3 only the diagram Fig. 3(c) survives to leading order in the large proton mass expansion in the physical gauge of a real photon. Secondly, we have decomposed the contribution of the diagram Fig. 3(c) into invariant and noninvariant parts with respect to a gauge transformation of a photon Green function $D_{\alpha\beta}(q) \to D_{\alpha\beta}(q) + c(q^2)q_\alpha q_\beta$. Finally, we have omitted a gauge-noninvariant part and the contributions, independent of the electron and photon energies, we have removed by renormalization of the Fermi weak coupling constant G_F and the axial coupling constant λ, respectively. The contribution of the diagrams in Figs. 3 and 4 to the branching ratio of the neutron radiative β^-–decay, obtained in such a way, is of order 10^{-4} (see Table I).

It is important to emphasize that the renormalized contribution of the diagram Fig. 3(c), which we have defined in terms of the functions $f_1(E_e, \vec{k}_e, \omega, \vec{k})$ and $f_2(E_e, \vec{k}_e, \omega, \vec{k})$ [see Eq. (C-33) of the Supplemental Material [20]], does not depend on the infrared cutoff μ, which is introduced as a photon mass [5]. This is unlike the contribution of the diagram Fig. 6(a) to the rate of the neutron β^- decay, which has been found as a function of the infrared cutoff μ [5]. A μ dependence of the radiative corrections, caused by the diagram Fig. 6(a), has been canceled only by the diagram Fig. 1(b) (see [5]).

We would like to accentuate that the contribution of the diagrams in Fig. 5, describing a neutron radiative β^- decay with two real photons in the final state, is also infrared stable. Having integrated over the momentum and energy of one of two photons we have obtained the contribution of order $O(\alpha^2/\pi^2)$ to the rate of the neutron radiative β^- decay with a photon, detected in the energy region $\omega_{\min} \leq \omega \leq \omega_{\max}$. The contribution of the neutron radiative β^- decay with two real photons in the final state, described by the diagrams in Fig. 5, is of order 10^{-5} (see Table I).

Total contributions of the radiative corrections of order $O(\alpha/\pi)$ to the rate of the neutron radiative β^- decay are about 2.42%, 2.44% and 3.66% for three photon-energy regions 15 keV $\leq \omega \leq$ 340 keV, 14 keV $\leq \omega \leq$ 782 keV and 0.4 keV $\leq \omega \leq$ 14 keV, respectively. They are commensurable with the radiative correction 3.75% to the rate of the neutron β^- decay [5,10]. However, they are not enhanced with respect to the contribution of the radiative corrections to the rate of the neutron β^- decay as we have expected because of an enhancement of the corrections of order $1/M$, caused by the weak magnetism and proton recoil [15]. The theoretical values of the branching ratios (see Table I) do not contradict the experimental data within the experimental error bars. Nevertheless, deviations of about 4.21%, 7.05% and 9.52% of the mean values of the experimental data from the theoretical values for three photon-energy regions 15 keV $\leq \omega \leq$ 340 keV, 14 keV $\leq \omega \leq$ 782 keV and 0.4 keV $\leq \omega \leq$ 14 keV, respectively, might only imply that such a distinction cannot be covered by the contributions of interactions beyond the Standard Model. Therefore, apart from the experimental error bars one may expect a better agreement between theory and experiment only from the contributions of strong low–energy interactions of hadrons beyond the axial coupling constant λ. One may expect that they might be caused by the contributions of diagrams in Fig. 4, where real and virtual photons couple to a hadronic block.

In this connection we may confess that there are two problems in our precision analysis of the rate of the neutron radiative β^- decay to order $O(\alpha^2/\pi^2)$. They are (i) a justification of a neglect of the diagrams with photons coupled to hadronic blocks such as the diagram Fig. 1(c) and so on and (ii) a justification of Sirlin's assumption for an extraction of a physical contribution from the Feynman diagrams in Figs. 3 and 4. As we have mentioned above both of these problems can be investigated only by a model-dependent way within certain models of strong low-energy interactions of hadrons coupled to photons.

However, it is very likely that the contribution of the diagram Fig. 1(c) is really not important. One may show this at the tree level using the following effective low-energy electromagnetic interactions of the neutron and proton [18]

$$\delta\mathcal{L}_{\rm em}(x) = \frac{\kappa_n e}{4M}\bar{\psi}_n(x)\sigma_{\mu\nu}\psi_n(x)F^{\mu\nu}(x) + \frac{\kappa_p e}{4M}\bar{\psi}_p(x)\sigma_{\mu\nu}\psi_p(x)F^{\mu\nu}(x), \quad (16)$$

where $\kappa_n = -1.91304$ and $\kappa_p = 1.79285$ are anomalous magnetic moments of the neutron and proton [26], respectively, and $\sigma_{\mu\nu} = (i/2)(\gamma_\mu\gamma_\nu - \gamma_\nu\gamma_\mu)$ are Dirac matrices [18]. The contribution of the diagram Fig. 1(c) to the amplitude of the neutron radiative β^- decay is equal to

$$\mathcal{M}_{\rm Fig.1c}(n \to pe^-\bar{\nu}_e\gamma)_{\lambda'} = -\frac{\kappa_n}{2M}\left[\bar{u}_p(\vec{k}_p,\sigma_p)\gamma^\mu(1+\lambda\gamma^5)\frac{1}{m_n - \hat{k}_n + \hat{k} - i0}i\sigma_{\alpha\beta}k^\alpha\varepsilon^{\beta *}_{\lambda'}u_n(\vec{k}_n,\sigma_n)\right] \times \left[\bar{u}_e(\vec{k}_e,\sigma_e)\gamma_\mu(1-\gamma^5)v_\nu\left(\vec{k}_\nu,+\frac{1}{2}\right)\right] + \frac{\kappa_p}{2M}\left[\bar{u}_p(\vec{k}_p,\sigma_p)i\sigma_{\alpha\beta}k^\alpha\varepsilon^{\beta *}_{\lambda'}\gamma^\mu(1+\lambda\gamma^5) \times \frac{1}{m_n - \hat{k}_p - \hat{k} - i0}u_n(\vec{k}_n,\sigma_n)\right]\left[\bar{u}_e(\vec{k}_e,\sigma_e)\gamma_\mu(1-\gamma^5)v_\nu\left(\vec{k}_\nu,+\frac{1}{2}\right)\right]. \quad (17)$$

One may see that the amplitude Eq. (17) is invariant under a gauge transformation $\varepsilon^*_{\lambda'}(k) \to \varepsilon^*_{\lambda'}(k) + ck$. The contribution of the diagram Fig. 1(c) to the branching ratio is given by

$$B^{\rm (Fig.1c)}_{\beta\gamma}(\omega_{\rm max},\omega_{\rm min}) = \frac{\alpha}{\pi}\frac{G_F^2|V_{ud}|^2}{2\pi^3 M}(2\lambda^2(\kappa_p+\kappa_n) - \lambda(\kappa_p-\kappa_n)) \times \int_{\omega_{\rm min}}^{\omega_{\rm max}} d\omega\omega\int_{m_e}^{E_0-\omega} dE_e\sqrt{E_e^2-m_e^2}(E_0-E_e-\omega)^2F(E_e,Z=1). \quad (18)$$

For the three photon-energy regions (see Table I) the branching ratio is equal to $B^{\rm (Fig.1c)}_{\beta\gamma} = 0.97\times10^{-10}$, $B^{\rm (Fig.1c)}_{\beta\gamma} = 1.25\times10^{-10}$ and $B^{\rm (Fig.1c)}_{\beta\gamma} = 4.90\times10^{-13}$, respectively. This may testify that the diagram Fig. 1(c) can actually be neglected. Such a neglect does not violate invariance of the diagrams Figs. 1(a) and 1(b) with respect to a gauge transformation $\varepsilon^*_{\lambda'}(k) \to \varepsilon^*_{\lambda'}(k) + ck$. Our justification of a possible neglect of the contribution of the diagram Fig. 1(c) confirms also a neglect of all diagrams with emission of a real photon by a hadronic block in the radiative neutron β^- decay with two real photons in the final state, given by the diagram in Fig. 5.

Hence, the main contribution of strong low-energy interactions we may expect only from the diagrams in Figs. 3 and 4. As a first step on the way of the analysis of

these diagrams we are planning to use the Standard Model of electroweak interactions supplemented by the linear σ model of strong low-energy nucleon-pion interactions by Gell-Mann and Levy [30] (see also [31]). It is well known that a linear σ model is a renormalizable one [32–34]. Renormalization of an extended version of a linear σ model has been investigated in [35,36]. The observed peculiar properties of strong low-energy hadronic interactions in the neutron radiative β^- decay to order of $O(\alpha^2/\pi^2)$ agree well with the assertion, pointed out by Weinberg [24], about the important role of strong low-energy hadronic interactions in decay processes.

We would like to emphasize that analysis of the rate of the neutron radiative β^- decay to order $O(\alpha^2/\pi^2)$ is a first step toward the analysis of the neutron β^- decay to order $O(\alpha^2/\pi^2)$. One of the most intriguing theoretical features of this analysis, which we anticipate, is a cancellation of the infrared dependences in the sum of the contributions of the diagrams with only virtual photon exchanges and the diagrams of the neutron radiative β^- decay with one and two photons in the final state. For the analytical investigation of this problem the results, obtained in this paper, are of great importance. The calculation of the neutron β^- decay to order $\alpha^2/\pi^2 \sim 10^{-5}$ together with the contributions of order $(\alpha/\pi)(E_e/M) \sim 3 \times 10^{-6}$ and $E_e^2/M^2 \sim 10^{-6}$ should give a new level of theoretical precision for the experimental search of interactions beyond the Standard Model [10].

It is well known that in the limit $m_\sigma \to \infty$, where m_σ is a scalar σ–meson mass, a linear σ–model is equivalent to current algebra [37,38]. This means that the results, obtained in a linear σ–model and taken in the limit $m_\sigma \to \infty$, should reproduce the results, obtained in current algebra [37,38], i.e. in a model–independent approach. This bridges between the results, which we are planning to obtain for the contributions of strong low–energy interactions to the radiative corrections of order $O(\alpha^2/\pi^2)$ for the neutron radiative and neutron β^- decays, and the results, obtained by Sirlin [5,23] for the contributions of strong low–energy interactions to the radiative corrections of order $O(\alpha/\pi)$ for the neutron β^- decay.

ACKNOWLEDGMENTS

The work of A. N. I. was supported by the Austrian "Fonds zur Förderung der Wissenschaftlichen Forschung" (FWF) under Contracts No. I689-N16, No. I862-N20, No. P26781-N20, and No. P26636-N20; "Deutsche Förderungsgemeinschaft" (DFG) AB 128/5-2; and by the ÖAW within the New Frontiers Groups Programme, NFP 2013/09. The work of R. H. was supported by the Erwin Schrödinger Fellowship program of the Austrian Science Fund FWF under Contract No. J3425-N27. The work of M. W. was supported by the MA 23 (FH-Call 16) under the project "Photonik-Stiftungsprofessur für Lehre."

[1] S. M. Berman, Radiative corrections to muon and neutron decay, Phys. Rev. **112**, 267 (1958).
[2] T. Kinoshita and A. Sirlin, Radiative corrections to fermi interactions, Phys. Rev. **113**, 1652 (1959).
[3] S. M. Berman and A. Sirlin, Some considerations on the radiative corrections to muon and neutron decay, Ann. Phys. (N.Y.) **20**, 20 (1962).
[4] G. Källén, Radiative corrections to β-decay and nucleon form factors, Nucl. Phys. **B1**, 225 (1967).
[5] A. Sirlin, General properties of the electromagnetic corrections to the beta decay of a physical nucleon, Phys. Rev. **164**, 1767 (1967).
[6] E. S. Abers, D. A. Dicus, R. E. Norton, and H. R. Queen, Radiative corrections to the fermi part of strangeness-conserving β decay, Phys. Rev. **167**, 1461 (1968).
[7] R. T. Shann, Electromagnetic effects in the decay of polarized neutrons, Nuovo Cimento A **5**, 591 (1971).
[8] Y. V. Gaponov and R. U. Khafizov, Yad. Fiz. **59**, 1270 (1996) [Phys. At. Nucl. **59**, 1213 (1996)]; Radiative neutron β-decay and its possible experimental realization, Phys. Lett. B **379**, 7 (1996); The radiative beta-decay mode of the free neutron, Nucl. Instrum. Methods Phys. Res., Sect. A **440**, 557 (2000).
[9] V. Bernard, S. Gardner, U.-G. Meißner, and C. Zang, Radiative neutron β-decay in effective field theory, Phys. Lett. B **593**, 105 (2004); Erratum, Phys. Lett. B **599**, 348(E) (2004).
[10] A. N. Ivanov, M. Pitschmann, and N. I. Troitskaya, Neutron β^- decay as a laboratory for testing the standard model, Phys. Rev. D **88**, 073002 (2013).
[11] A. N. Ivanov, R. Höllwieser, N. I. Troitskaya, and M. Wellenzohn, Proton recoil energy and angular distribution of neutron radiative β^- decay, Phys. Rev. D **88**, 065026 (2013).
[12] J. S. Nico *et al.*, Observation of the radiative decay mode of the free neutron, Nature (London) **444**, 1059 (2006).
[13] R. L. Cooper *et al.*, Radiative β decay of the free neutron, Phys. Rev. C **81**, 035503 (2010).
[14] M. J. Bales *et al.* (RDK II Collaboration), Precision Measurement of the Radiative β Decay of the Free Neutron, Phys. Rev. Lett. **116**, 242501 (2016).
[15] A. N. Ivanov, R. Höllwieser, N. I. Troitskaya, M. Wellenzohn, and Ya. A. Berdnikov, Precision theoretical analysis of neutron radiative beta decay, Phys. Rev. D **95**, 033007 (2017).
[16] S. Gardner and D. He, T-odd momentum correlation in radiative β decay, Phys. Rev. D **86**, 016003 (2012); T-odd

momentum correlation in radiative β decay, Hyperfine Interact. **214**, 71 (2013).
[17] S. Gardner and D. He, Radiative β decay for studies of *CP* violation, Phys. Rev. D **87**, 116012 (2013).
[18] C. Itzykson and J.-B. Zuber, in *Quantum Field Theory* (McGraw-Hill Inc., New York, 1980).
[19] A. N. Ivanov, Ambiguity of the muon anomalous magnetic moment in gauge—invariant theories, Yad. Fiz. **18**, 1283 (1973).
[20] See Supplemental Material at http://link.aps.org/supplemental/10.1103/PhysRevD.95.113006 for detailed calculations of the Feynman diagrams in Figs. 1–5 and discuss the properties of these diagrams with respect to gauge transformations of the wave functions of real photons and photon Green functions.
[21] J. D. Bjorken and S. D. Drell, in *Relativistische Quantenfeldtheorie* (Bibliographisches Institut Mannheim, Hochschultaschenbücher-Verlag, Frankfurt am Main, 1967).
[22] A. N. Ivanov, R. Höllwieser, N. I. Troitskaya, M. Wellenzohn, O. M. Zherebtsov, and A. P. Serebrov, Deficit of reactor antineutrinos at distances smaller than 100 m and inverse β decay, Phys. Rev. C **88**, 055501 (2013).
[23] A. Sirlin, Current algebra formulation of radiative corrections in gauge theories and the universality of the weak interactions, Rev. Mod. Phys. **50**, 573 (1978); Erratum, Rev. Mod. Phys. **50**, 905(E) (1978).
[24] S. Weinberg, Role of strong interactions in decay processes, Phys. Rev. **106**, 1301 (1957).
[25] H. Abele, The neutron. Its properties and basic interactions, Prog. Part. Nucl. Phys. **60**, 1 (2008).
[26] C. Partignani *et al.* (Particle Data Group Collaboration), Review of particle physics, Chin. Phys. C **40**, 100001 (2016).
[27] S. Weinberg, in *Foundations*, The Quantum Theory of Fields Vol. I (Cambridge University Press, New York, 1995), p. 472.
[28] N. N. Bogoliubov and D. V. Shirkov, in *Introduction to the Theory of Quantum Fields* (Interscience Publishers, Inc., New York, 1959).
[29] R. Pohl *et al.*, The size of the proton, Nature (London) **466**, 213 (2010).
[30] M. Gell-Mann and M. Levy, The axial vector current in beta decay, Nuovo Cimento **16**, 705 (1960).
[31] V. De Alfaro, S. Fubini, G. Furlan, and C. Rossetti, in *Currents in Hadronic Physics* (North-Holland Publishing Company, Amsterdam, 1973).
[32] J. Bernstein, M. Gell-Mann, and L. Michel, On the renormalization of the axial vector coupling constant in β-decay, Nuovo Cimento **16**, 560 (1960).
[33] K. J. Kim, The renormalized σ model, Ann. Phys. (N.Y.) **79**, 287 (1973).
[34] A. S. Johnson, J. A. McNeil, and J. R. Shepard, Renormalization group flow equations for the sigma model, Phys. Rev. D **58**, 014001 (1998).
[35] R. D. Pisarski and F. Wilczek, Remarks on the chiral phase transition in chromodynamics, Phys. Rev. D **29**, 338 (1984).
[36] M. Grahl and D. H. Rischke, Functional renormalization group study of the two-flavor linear sigma model in the presence of the axial anomaly, Phys. Rev. D **88**, 056014 (2013).
[37] S. Weinberg, Dynamical Approach to Current Algebra, Phys. Rev. Lett. **18**, 188 (1967).
[38] S. Gasiorowicz and D. A.Geffen, Effective lagrangians and field algebras with chiral symmetry, Rev. Mod. Phys. **41**, 531 (1969).